Hindawi
Advances in Materials Science and Engineering
Volume 2018, Article ID 2780203, 12 pages
https://doi.org/10.1155/2018/2780203

Research Article

Optical CO_2 Gas Sensing Based on TiO_2 Thin Films of Diverse Thickness Decorated with Silver Nanoparticles

Muhammad Akram Raza,[1] **Anam Habib**,[1] **Zakia Kanwal**,[2] **Syed Sajjad Hussain**,[1] **Muhammad Javaid Iqbal**,[1] **Murtaza Saleem**,[3] **Saira Riaz**,[1] **and Shahzad Naseem**[1]

[1]*Centre of Excellence in Solid State Physics, University of the Punjab, Lahore 54590, Pakistan*
[2]*Department of Zoology, Lahore College for Women University, Jail Road, Lahore 54000, Pakistan*
[3]*Department of Physics, School of Science and Engineering (SSE), Lahore University of Management Science (LUMS), Lahore, Pakistan*

Correspondence should be addressed to Muhammad Akram Raza; akramraza.cssp@pu.edu.pk

Received 26 March 2018; Revised 29 May 2018; Accepted 14 June 2018; Published 19 July 2018

Academic Editor: Mikhael Bechelany

The fabrication, characterization, and CO_2 gas detection performance of single component-based and hetero-nanostructure-based optical gas sensors are reported in the present work. Single component-based structures include (i) TiO_2 thin films with varied film thickness (37.45 nm, 51.92 nm, and 99.55 nm) fabricated via the RF sputtering system for different deposition times and (ii) silver nanoparticles (AgNPs) deposited on the glass substrate by the wet chemical method. Hetero-nanostructures were achieved by decorating the AgNPs on the predeposited TiO_2 thin films. The structural, morphological, and optical characteristics of prepared samples were studied by X-ray diffraction (XRD), scanning electron microscopy (SEM), and ellipsometry, respectively. XRD analysis of AgNPs confirmed the crystalline nature of prepared particles with average crystallite size of 21 nm, however, in the case of TiO_2 films XRD results suggested amorphous structure of all as-deposited films. size 21 nm. The SEM micrographs confirmed the deposition of AgNPs on the TiO_2 thin films. With increasing sputtering time, TiO_2 films were found to be denser and more compact, indicating a reduced porosity and higher film thickness. CO_2 gas-sensing properties were investigated by measuring the optical transmission spectra in alone air and in CO_2 gaseous atmosphere at room temperature. It was observed that neither TiO_2 thin films even with higher thickness nor alone AgNPs could demonstrate any substantial gas-sensing activity. Nevertheless, TiO_2/AgNP hetero-nanostructured substrates exhibited excellent CO_2 gas-sensing performance as indicated by a huge change in the transmission spectra. The enhanced sensing efficiency of TiO_2/AgNP nanostructures owing to synergistic effects suggests a promising role of our manufactured sensors in practical applications.

1. Introduction

To meet the needs of rapidly increasing human population, industry production has drastically increased. During this process, a lot of industrial waste is causing environmental pollution due to improper disposal and management. The most common forms of industrial contaminants are pollutant gases such as CO, C_6H_4, NO_x, NH_3, CH_4, SO_2, and CO_2. The exhaust fumes from automobiles are further intensifying the quantity of such pollutants in air making them more toxic and harmful for humans and for the natural ecosystem [1, 2]. The increasing public health issues demand strong efforts to reduce the impact of these noxious gases. The development of efficient sensors for gas monitoring could be the first step to address this challenge.

For the quantitative detection of various gases in the environment, different types of traditional gas sensors are used including pellistors, semiconductor devices, and electrochemical gas sensors. Although these sensors are widely employed in several applications, they suffer from different drawbacks. For example, pellistors being robust in nature respond to combustion on a catalyst bead. They are suitable for flammable gases detection around the lower explosive limit but face zero drift problems at parts per

million (ppm) levels. Semiconductor gas sensors can work effectively at the low ppm levels; however, they also suffer from drift and humidity variations and cross-respond to other gases. Similarly, electrochemical gas devices can be sensitive at ppm or ppb levels and comparatively explicit to individual gases; nevertheless, they have issues such as limited lifetimes, known cross-response, and changing humidity levels [3, 4].

Owing to aforementioned limitations and drawbacks of conventional gas-sensing devices, optical gas sensors are attracting more attention. They are based on materials that can change their optical response when exposed to target gaseous atmosphere. They are fast in action (even below 1 sec) and have negligible drift and high gas specificity, with minimal cross-response. They provide a wide range of operative parameters, and any change in intensity, frequency, polarization, and phase of reflected or transmitted light as compared to incident light can be used in the sensing mechanism. Measurements made by optical gas sensors are self-referenced and inherently reliable because the intensity of incident and transmitted/reflected light can be determined. Furthermore, contactless readout measurements and independency from electromagnetic noise make them suitable for optical fibers and integrated photonic devices for possibly fast and easy signal transport and in situ measurements with a compact, flexible system [1, 5, 6].

Carbon dioxide (CO_2), a colorless, generally inert in nature, and highly oxidizing gas, belongs to those greenhouse gases that occur both naturally (by decomposition of organic matter) and from human activities (including burning fossil fuels for power generation, oil refining, natural gas production, and transportation). Higher concentration of CO_2 in the atmosphere is not only dangerous for living beings but also has severe impact on global climate. For example, maximum limit of CO_2 required by safety regulations in a mixture of gases for mines, wells, and sewers operations is 5–20%. Beyond this limit, it becomes hazardous for humans health. Likewise, the anomalous increase of CO_2 can cause huge global climate changes such as greenhouse effect, global warming, possible expansion of subtropical deserts, and increase in sea levels [7–9]. Therefore, the qualitative and quantitative detection of CO_2 is of substantial interest in various fields such as biotechnology, food packaging and beverage, marine and environmental science, medicine and health, air quality, and industrial monitoring [10, 11].

Titanium dioxide (TiO_2) owing to low cost, low oxidation potential, and nontoxic in nature along with high refractive index, high dielectric constant, and chemical stability is of much interest in various applications such as catalysis, optoelectronic devices, photocatalysis, and sensors [12–14]. TiO_2-based gas sensors are becoming popular for their potential use in medicine, biology, self-safety, transportation industries, and environmental protection purposes [15, 16]. To improve the sensing performance of these sensors, various techniques have been employed by the researchers. Manufacturing of TiO_2-based heteronanostructures using the metallic nanoparticles is a promising approach in the gas-sensing mechanism. The combined effect of the functional TiO_2 matrix and large active surface areas of nanoparticles could boost the sensing efficiency as compared to single component-based sensors [15, 17, 18].

The aim of this work was to explore the synergistic effect of TiO_2/AgNP hetero-nanostructures for CO_2 gas sensing. TiO_2 thin films of varied thickness were fabricated via the RF magnetron sputtering system, and AgNPs were decorated on them by the wet chemical method. The optical CO_2 gas detection experiments were carried out by measuring the transmission signals in a normal incident configuration of a variable-angle ellipsometer at room temperature. CO_2 gas-sensing performance of alone AgNP films, pristine TiO_2 thin films having different thickness, and AgNP-loaded TiO_2 films was investigated. The effect of enhanced TiO_2 film thickness on the AgNP deposition and CO_2 gas-sensing efficacy was also studied. The focus of this study was to work out the best possible composite morphology for most effective and reliable CO_2 gas sensors.

2. Materials and Methods

2.1. Preparation of Samples. Three types of substrates were prepared: (i) alone TiO_2 thin films having thickness of 37.45 nm, 51.92 nm, and 99.55 nm, (ii) alone silver nanoparticles deposited on glass substrates, and (iii) TiO_2/AgNP hetero-nanostructure substrates with varied above-mentioned TiO_2 film thickness. Titanium dioxide (TiO_2) thin films were fabricated on soda lime glass substrates via the RF magnetron sputtering technique. The glass slides were cleaned ultrasonically for 20 min first in acetone and then for further 20 min in IPA and dried in nitrogen (N_2) flow, prior to film deposition. TiO_2 films were sputtered using the titanium dioxide target, in the argon (Ar) environment with a fixed flow rate of 50 sccm at room temperature and 10^{-6} Pa of pressure. To achieve a varied film thickness, the deposition time was changed as 30 min, 60 min, and 90 min, keeping all other parameters unchanged. The TiO_2 thin film samples were used as-deposited without any annealing for further application.

In the next step, deposition of sliver nanoparticles (AgNPs) was carried out on bare glass substrates and on TiO_2 thin film samples. AgNPs were first synthesized following a chemical reduction route described in detail in our previous study [19]. Briefly, 100 mL of 1 mM aqueous solution of silver nitrate ($AgNO_3$) was heated to boiling temperature under vigorous stirring and refluxing conditions. Then, 10 mL of aqueous solution of 1% trisodium citrate ($Na_3C_6H_5O_7$) was added dropwise with the help of a dropper. The solution changed color from transparent color to pale yellow to bright yellow and finally to greenish yellow, indicating the completion of the reaction as shown in Figure 1. Dissolving of silver precursors produced silver ions (Ag^+) in the aqueous solution. These Ag^+ ions were reduced to free silver atoms (Ag^0) by the reducing agent (trisodium citrate) which resulted in the initial color change (pale yellow). Owing to nucleation and growth processes, produced free silver atoms (Ag^0) gathered into the oligomeric clusters and finally into silver nanoparticles [20]. The color change from bright yellow to greenish yellow indicated the

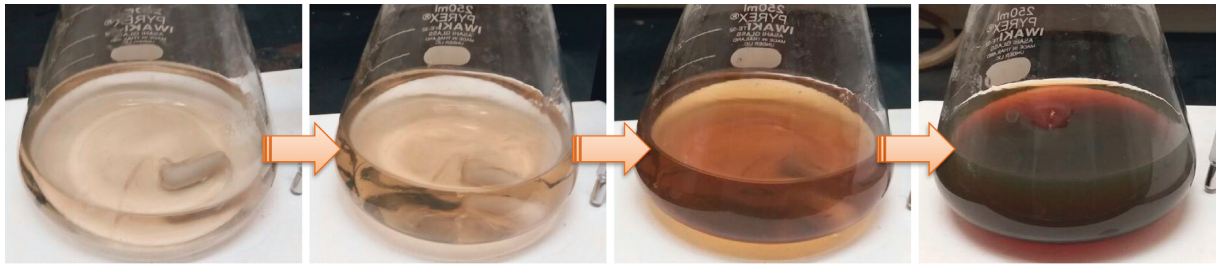

(a) (b) (c) (d)

Figure 1: Color change during the synthesis of AgNPs depicting different stages of the reaction. (a) Dissolving of silver precursors into water remained transparent. (b–d) Introduction of the reducing agent (trisodium citrate) caused the reduction of precursors as appeared in color change from transparent to greenish yellow.

different phases taking place in the reaction. Trisodium citrate served as a reducing agent and a stabilizing agent in this case. The colloidal solution was cooled to room temperature for further characterization and applications.

Before decorating with AgNPs, all substrates (bare glass and TiO_2 thin films) were functionalized with 3-aminopropyltriethoxysilane (APTES) to obtain a high surface affinity for the colloidal AgNPs adopting a solution-based approach [21]. Briefly, bare cleaned glass substrates and TiO_2 film samples were immersed into a 10% APTES methanolic solution for 60 min, followed by thoroughly rinsing with pure methanol and drying in N_2 flow. Then, the samples were immersed in water for 30 min and dried in N_2 flow after rinsing with water. Finally, APTES-derivatized substrates were immersed in the silver colloidal suspension for the whole night, rinsed with water, and dried in N_2 flow. All of these procedures were performed at room temperature.

2.2. Characterization of Prepared Samples. All three types of fabricated samples were characterized with different characterization techniques for their morphological, optical, and structural analyses. Structural investigations were carried out by using X-ray diffraction (XRD) methods with an X-ray diffractometer (D-MaxIIA; Rigaku, Tokyo, Japan) operated at 40 kV and 25 mA using Cu Kα line radiation ($\lambda = 1.5406$ Å). Few drops of the silver colloidal sample were dried on the clean glass substrate to form a thick film for XRD measurements. A field-emission scanning electron microscope (FEI Nova NanoSEM 450; Hillsboro, USA) was used to study the morphology of obtained structures at different magnifications. A thin gold layer (10 nm) was also deposited, if needed, to avoid any possible charging on the sample. The thickness and the optical constants of TiO_2 thin films fabricated at different deposition times were determined by spectroscopic ellipsometry. The measurements were carried out using a variable-angle ellipsometer (M-2000; J.A. Woollam, USA) in air (without chamber) at a fixed incidence angle of 65° with respect to the surface normal operating in the wavelength range of 300–900 nm at room temperature.

2.3. Optical Gas Sensing. In order to examine the optical CO_2 gas-sensing performance of all three aforementioned categories of samples, optical transmission measurements were performed (in air and in CO_2 gas) within a custom-made transparent airtight gas-sensing chamber (8 cm × 6 cm × 12 cm) using a spectroscopic ellipsometer in the vertical configuration (as shown in Figure 2) in the wavelength (λ) range of 300 nm to 900 nm at room temperature. CO_2 gaseous environment was established by a constant flow rate of 50 sccm. Measurements were carried out by exposing each sample to air and to CO_2 gaseous atmosphere for 2 min.

The light beam was allowed to fall on the substrate at right angle (as schematically shown in Figure 2) which covered an area of about 2.8 mm^2 on the substrate. The change in transmission due to CO_2 gas was recorded for each sample.

3. Results and Discussion

Figure 3 shows TiO_2 thin film samples before and after AgNP deposition as an upper panel and a lower panel, respectively. It can be seen that the shade of the color changes from lighter to darker as the deposition times enhanced from 30 min to 90 min, which could be an indication of increased film thickness. After decorating with silver NPs, a further change in the color was noticed that depicts the successful adsorption of AgNPs.

3.1. X-Ray Diffraction Analysis. The crystalline nature of as-deposited TiO_2 thin films with sputtering times of 30 min, 60 min, and 90 min (without any further heat treatment) and synthesized AgNPs was determined by the XRD technique at room temperature.

The XRD indexed pattern of alone AgNPs deposited on the glass substrate by the drop-casting method is shown in Figure 4. Four major characteristic peaks at 2θ values of 38.45°, 46.35°, 64.75°, and 78.05° can clearly be observed. These peaks can be discerned to the reflection planes (111), (200), (220), and (311) of the face-centered cubic (FCC) pure metallic silver according to JCPDS file number 04-0784 [22]. Thus, XRD results confirmed the pure crystalline metallic nature of our synthesized AgNPs.

The broadening of the major diffraction peak (111) was utilized to calculate the crystallite size of prepared AgNPs using Debye–Scherrer's formula [23] as follows:

$$D = \frac{k\lambda}{\beta_{hkl} \cos \theta}, \quad (1)$$

where λ is the wavelength of X-ray used (1.54 Å), k is the shape factor (0.9), β_{hkl} (taken in radians) is the full width at

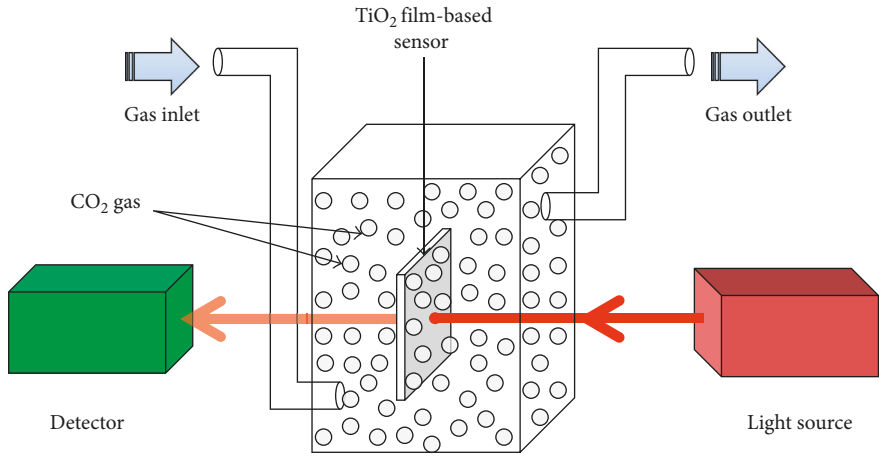

Figure 2: Experimental setup for CO_2 gas sensing.

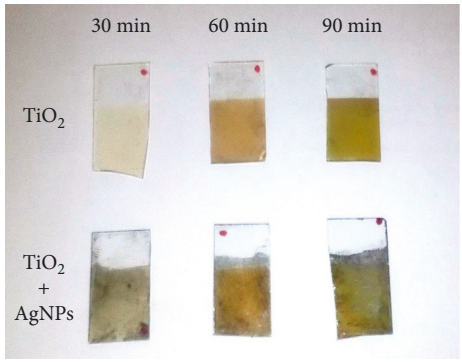

Figure 3: A CCD image showing the fabricated TiO_2 thin films on glass substrates before and after AgNP deposition.

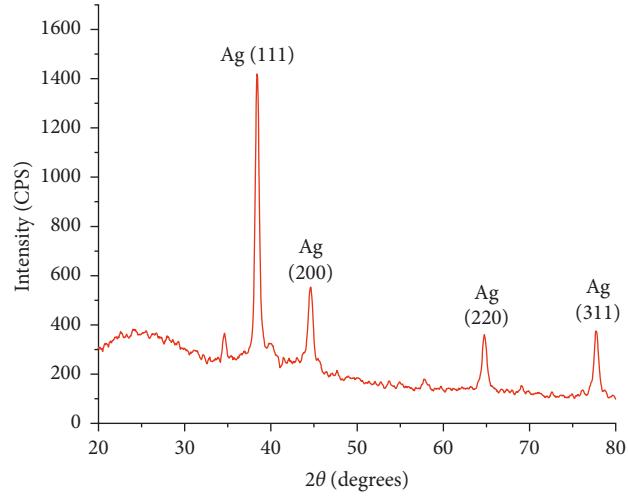

Figure 4: XRD pattern of the AgNP sample.

half maximum (FWHM) of the diffraction peak, and θ is the diffraction angle at that intensity. All measured vales are listed in Table 1. The average crystalline size of AgNPs was found to be 21 ± 1 nm as listed in Table 1.

The XRD spectra obtained for TiO_2 thin films for deposition times of 30 min, 60 min, and 90 min are shown in Figure 5(a). No sharp peak can be observed in all three spectra which can help to identify the crystalline nature or any phase of deposited TiO_2 films. Absence of any strong reflection peak revealed apparently the amorphous nature of as-deposited TiO_2 thin films in our case. This indicated that, without any further annealing or heat treatment, there was not enough crystalline structure developed which could be detected by the XRD. Perhaps, proper annealing could be helpful to develop sufficient crystalline nature of the films. However, a slight increase in the intensity of the spectra can be noticed by increasing the film deposition time which might be due to increased film thickness.

For the measurements of fabricated film thickness, refractive index, and film roughness, spectroscopic ellipsometry was employed, and calculations were made using the well-known Tauc–Lorentz oscillator model [24, 25]. The obtained results are presented in Figure 5(b) by plotting the refractive indices as a function of wavelength and are listed in Table 2. It can be observed that, by increasing the deposition time, TiO_2 film thickness, refractive index, and film roughness increased which can be attributed to enhanced atomic packing density and decrease in the porosity of the deposited film [25, 26].

3.2. Scanning Electron Microscopy Analysis. In order to determine the size and the shape of prepared AgNPs and the morphology of the TiO_2 thin films with and without AgNP deposition, a field-emission scanning electron microscope (FE-SEM) was used.

Figure 6 shows the SEM micrographs of AgNPs deposited on glass substrates (by drop-casting methods). It is evident from SEM images that shapes of the silver particles were not perfectly spherical, although some round-shaped particles can also be noticed in magnified view (Figure 6(a)). The size of synthesized particles was found in the range of 20 nm to 60 nm. The observed agglomeration and clustering of particles could be the result of depositing and drying processes of silver colloids on glass by the drop-casting method.

SEM images of TiO_2 thin films prepared at different deposition times (30, 60, and 90 min) on glass substrates with and without AgNPs are presented in Figure 7. It can be

Table 1: Calculated crystallite size of AgNPs.

Peak position (2θ)	Diffraction plane (hkl)	FWHM (radians)	Crystallite size D (nm)
38.45°	(111)	0.0069	21 ± 1

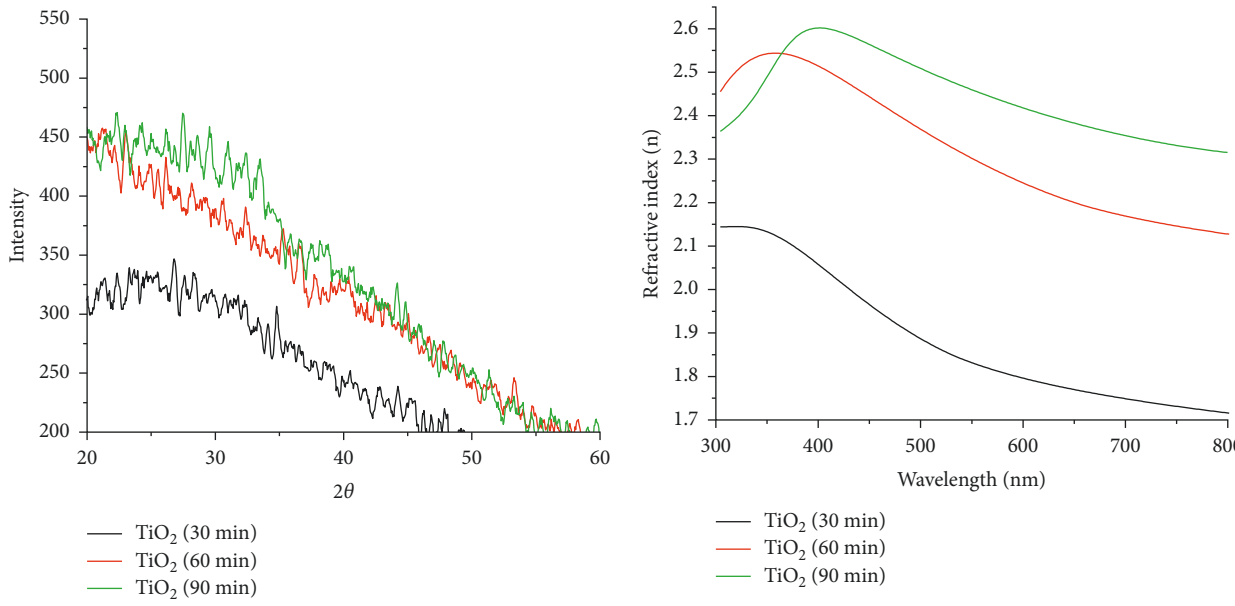

(a) (b)

Figure 5: XRD (a) and ellipsometry spectra (b) of TiO_2 thin films for different deposition times.

Table 2: Calculated refractive indices for different deposition times of TiO_2 thin films.

Film deposition time (min)	Refractive index (at $\lambda = 550$ nm)	Film thickness (nm)	Film roughness (nm)
30	1.832	37.54	0.02
60	2.301	51.92	6.05
90	2.459	99.55	8.81

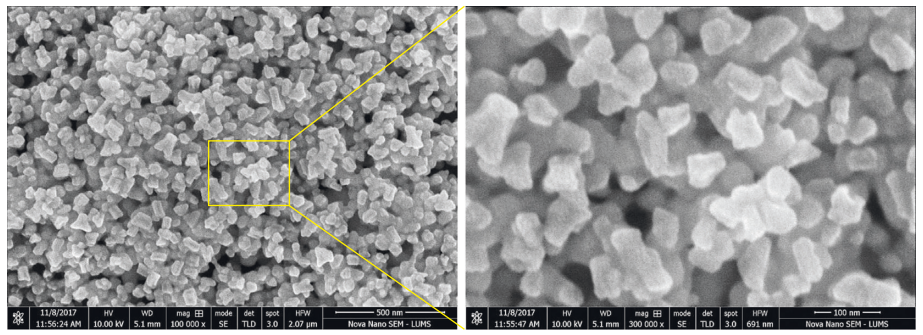

(a) (b)

Figure 6: SEM images of AgNPs at different magnifications.

observed that TiO_2 thin films with lower thickness (Figure 7(a)) comprised many islands of tiny particles having size in the range of 20 to 30 nm. At some places, TiO_2 cluster formation can also be observed, and the overall film structure seemed to be porous. After the deposition of AgNPs, the morphology of the substrate appeared as TiO_2 films decorated with randomly scattered clusters of AgNPs (Figure 7(b)).

For the TiO_2 samples with moderate film thickness of 51 nm (Figure 7(c)), it appeared that TiO_2 film became dense and compact, indicating the decreased porosity and enhanced film thickness. The occurrence of TiO_2 clusters at many places can also be noticed increasing the film roughness. The introduction of AgNPs (Figure 7(d)) over the 51 nm thick TiO_2 films depicted that density of scattered

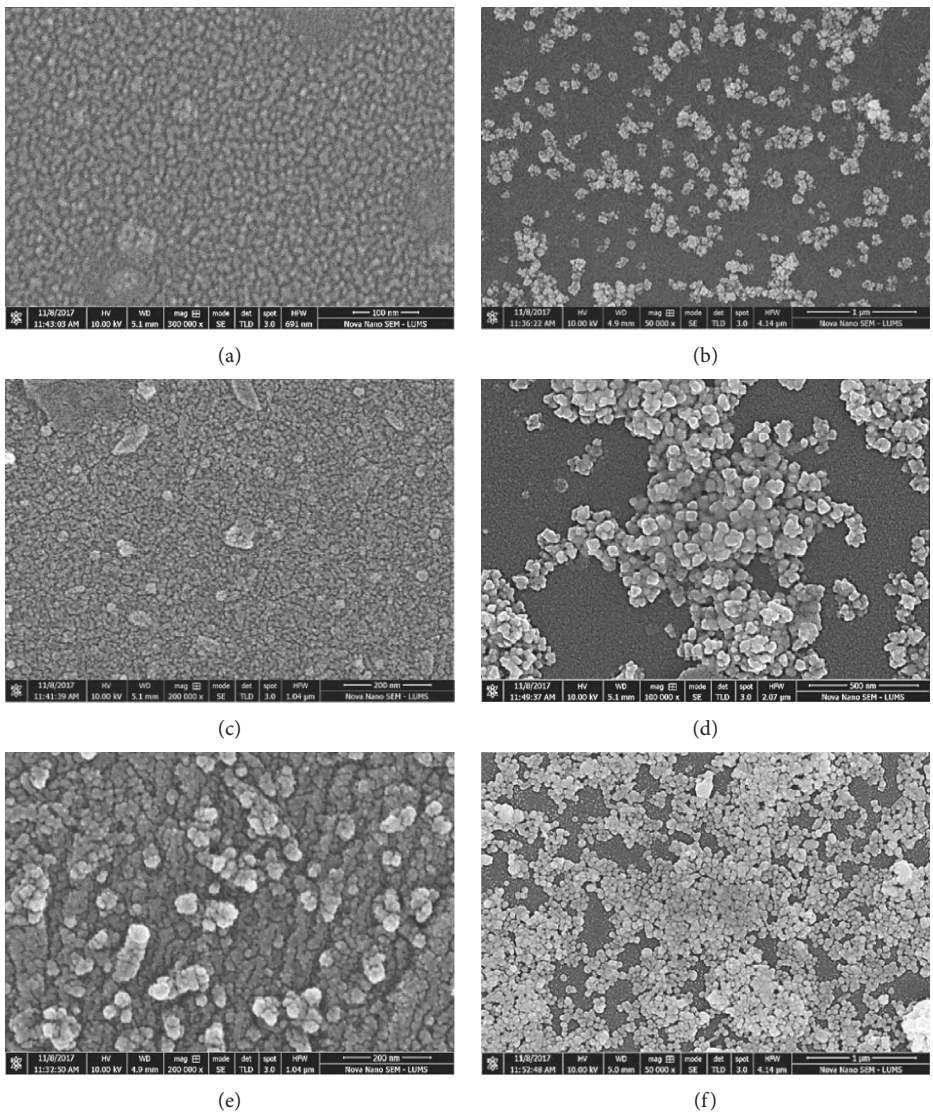

Figure 7: SEM micrographs of TiO_2 thin films having different thickness: (a) 37.54 nm, (c) 51.92 nm, and (e) 99.55 nm, without (left) and with AgNPs (right).

AgNP clusters appeared to increase. Perhaps, the agglomeration of AgNPs occurred over the already developed TiO_2 clusters which increased by increasing film deposition time. In the case of 90 min deposition time, the film thickness and roughness further increased, and more clusters and bump-like structures can be observed on the TiO_2 films (Figure 7(e)). The film morphology after depositing the AgNPs revealed that hill- and valley-like structures covered the TiO_2 films (Figure 7(f)).

The deposition of AgNPs in the form of clusters and bunches instead of uniform distribution of individual nanoparticles could be due to nonuniform adsorption of APTES layers on TiO_2 thin films by various chemisorption and physisorption mechanisms leading to scattered binding sites for AgNPs [27]. Besides, the formation of TiO_2 clusters in the films might be another reason of AgNP agglomeration during the deposition process that enhanced the manufactured structure roughness.

It can be concluded from the SEM results that, by increasing the film deposition times from 30 to 90 min, the film morphology clearly changed by improving the thickness and roughness of the deposited film. The deposition of AgNPs not only developed the hetero-nanostructures but also enhanced the roughness by nonuniform decoration of silver clusters and hill- and valley-like assemblies on TiO_2 films.

3.3. CO_2 Gas-Sensing Analysis. In order to describe the measured optical response of all the samples in the air and in CO_2 atmosphere, the substrates were divided into two categories:

(a) Substrates without silver nanoparticles (AgNPs)

(b) Substrates with silver nanoparticles (AgNPs).

3.3.1. Substrates without AgNPs. In Figure 8, transmission spectra of all four samples, bare glass and TiO_2 thin films, having different film thickness (37.54 nm, 51.92 nm, and

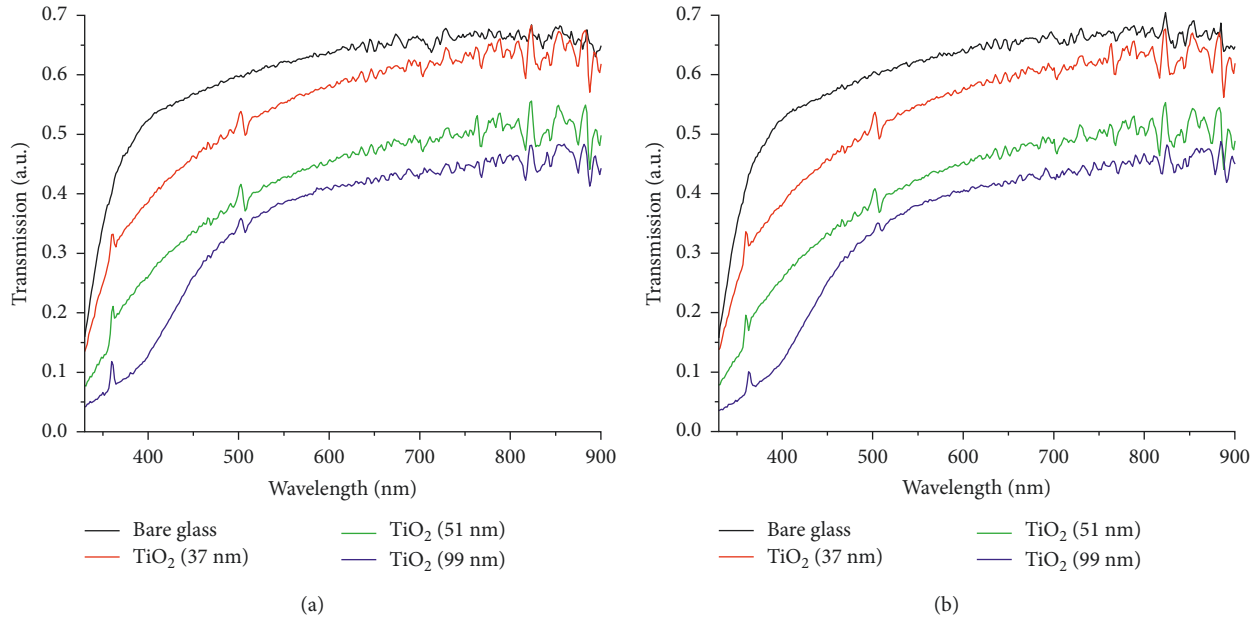

Figure 8: Transmission spectra of TiO_2 thin films with thickness of 37 nm, 51 nm, and 99 nm in air (a) and CO_2 gas flow (b).

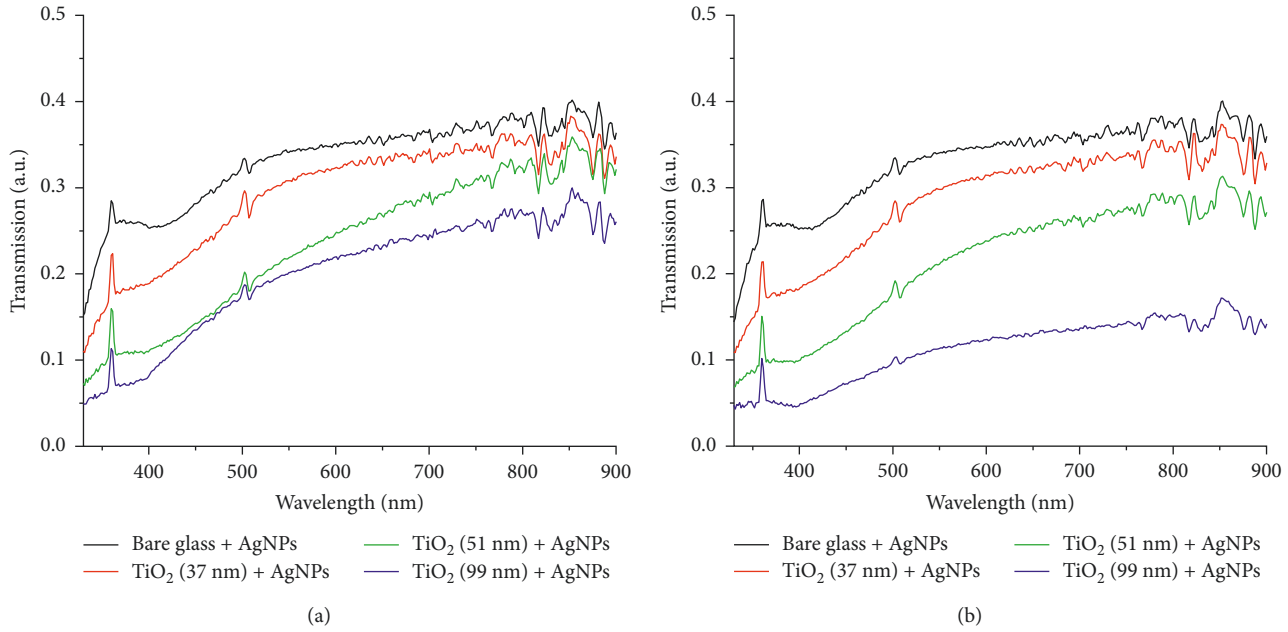

Figure 9: Transmission spectra of TiO_2 thin films decorated with AgNPs of varied film thickness in air (a) and CO_2 gas flow (b).

99.55 nm), in air and in the presence of CO_2, are presented. It can be seen that, in case of air (Figure 8(a)), bare glass exhibited the typical spectrum with maximum transmission. Apparently, the transmission value of the glass substrate (~60%) seems lower than the reported value (<90%) [28]. All optical measurements were carried out inside a transparent box to generate a gaseous environment around the sample (Figure 2). The lower values of the bare glass substrate might be due to reflections off the windows of the gas cell apparatus. For the TiO_2 thin film samples, transmission was found to decrease by increasing the film deposition. This can be understood by considering the improvement in the film thickness and density which absorbed more light causing a decrease in transmission. In the case of CO_2 gaseous atmosphere, transmission spectra (Figure 8(b)) of all four samples without AgNPs appeared similar to those as were in the case of alone air. Thus, no clear difference could be noticed in the presence of CO_2 gas.

3.3.2. Substrates with AgNPs. The optical transmission spectra of all samples decorated with AgNPs in air and in the presence of CO_2 gas are demonstrated in Figure 9. A slight

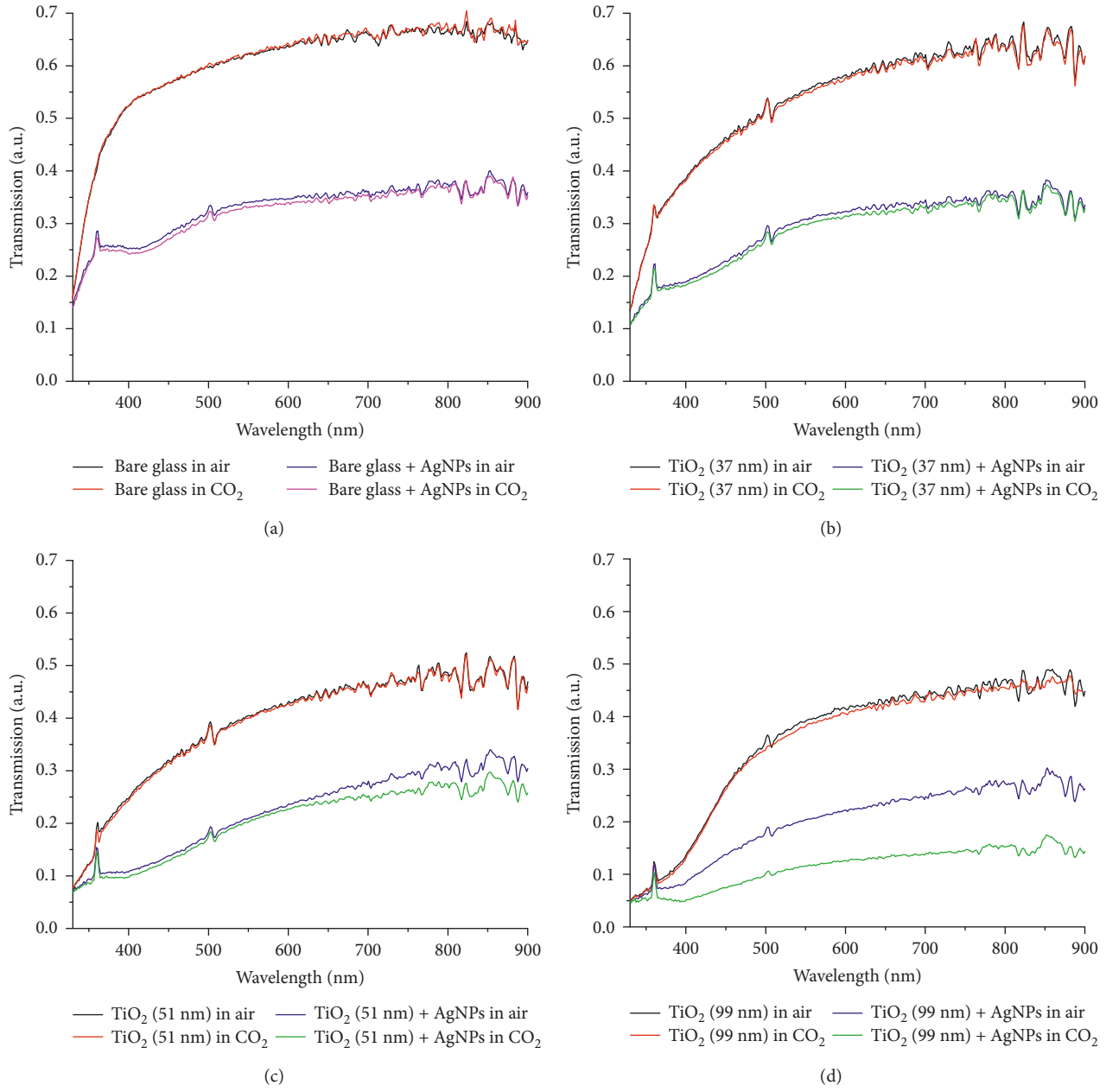

Figure 10: Comparison of optical responses of all samples in air and CO_2 gas flow.

change in the shape of all spectra can be noticed. As evident from SEM images (Figure 7), deposition of AgNPs formed different-sized Ag aggregates along with some scattered distinctive AgNPs. These Ag aggregates could act as scattering centers causing a decrease in the transmission signal which are discussed in the next section.

3.3.3. Comparison of Gas-Sensing Performance. A detailed comparison of optical characteristics in the presence and absence of CO_2 gaseous atmosphere for all samples is reported in Figure 10.

Figure 10(a) represents the transmission response of bare glass and alone AgNP-deposited glass substrate in air and in CO_2 gas flow. A huge decrease in the transmission spectra (in air) of the glass substrate decorated with AgNPs as compared to bare glass indicates the improved surface coverage of the glass substrate by the deposition of AgNPs. However, no significant change in the optical spectra due to the CO_2 gas atmosphere can be noticed except a slight decrease in case of AgNP-loaded samples. This revealed substrates covered with AgNPs alone were not sufficient enough for CO_2 gas detection.

In the case of TiO_2 thin film (37 nm thickness) samples with and without AgNP deposition (Figure 10(b)), the overall decrease in the optical response was found to be larger as compared to samples without TiO_2 films (Figure 10(a)). This depicts that morphology and thickness of the material on glass substrates had changed due to TiO_2

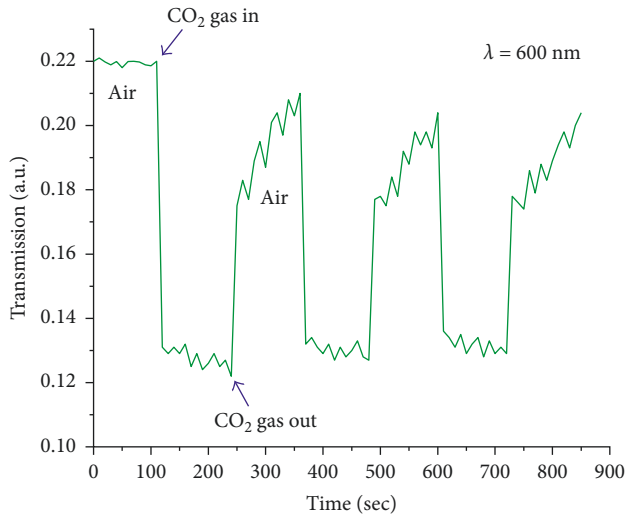

Figure 11: Dynamic CO_2 gas-sensing response of TiO_2 films decorated with AgNPs with maximum thickness (99 nm).

thin films. However, absence of any prominent change in the transmission in the CO_2 gaseous environment proved that TiO_2 thin films with insufficient thickness despite the presence of AgNPs were also incapable of noticeable CO_2 gas sensing.

For the TiO_2 samples with 51 nm film thickness (Figure 10(c)), a significant decrease in the transmission spectra, starting from 600 nm to higher wavelength values, was noticed when TiO_2 thin films decorated with AgNPs were exposed to CO_2 gas flow. This indicates that increased TiO_2 content in hetero-nanostructures (TiO_2/AgNPs) had improved the CO_2 gas-sensing properties of the samples. This argument was further strengthened when TiO_2 thin films of higher thickness (99 nm) loaded with AgNPs were analyzed in the CO_2 gaseous environment as shown in Figure 10(d). A huge decrease in the transmission of hetero-nanostructured samples exposed to CO_2 gas (green line) was noticed as compared to air alone (blue line). These optical results revealed that neither alone silver nanoparticles nor alone TiO_2 films of various thicknesses were proficient CO_2 gas sensors nevertheless; hetero-nanostructures (TiO_2/AgNPs) with higher TiO_2 content provided the maximum CO_2-sensing properties.

3.3.4. Dynamic Gas Sensing. Figure 11 illustrates the dynamic CO_2 gas-sensing response of the hetero-nanostructured sample TiO_2/AgNPs with maximum TiO_2 film thickness (99 nm). The transmission signal measurements were carried out at room temperature for a fixed wavelength ($\lambda = 600$ nm) by flowing air and CO_2 gas alternatively. The response time (air-to-CO_2 gas transient) is defined as the time required to achieve 10% to 90% of maximum transmission signal, while the recovery time (CO_2 gas-to-air transient) is defined as the time required to achieve 90% to 10% of maximum transmission. The response time was found to be about 10 sec, while recovery time was about 110 sec. The dynamic gas-sensing results (Figure 11) revealed the stability and reversibility of our prepared CO_2 gas sensors.

3.3.5. Transmission Change Ratio (TCR). The sensitivity of various samples toward CO_2 gas can more clearly be observed in Figure 12, which reports the calculated transmission change ratio (TCR) values. TCR is defined as the difference between the transmissions measured during CO_2 gas exposure (T_{gas}) and in air (T_{air}), normalized to the transmissions level in air, and is given by the following formula [17]:

$$\mathrm{TCR} = \frac{T_{gas} - T_{air}}{T_{air}}. \quad (2)$$

The TCR plots of substrates without AgNPs and with AgNPs are presented in Figures 12(a) and 12(b), respectively. The almost same behavior of TCR around zero line for all the samples without AgNPs (Figure 12(a)) indicates that increased TiO_2 film thickness alone was not enough to produce any sharp change in transmission as exposed to CO_2 gas. However, in the case of hetero-nanostructured morphology, a combination of TiO_2 thin films of higher thickness with AgNPs, a substantial variation in TCR trend was noted. A perturbation in TCR (blue line) of 51 nm thickness (TiO_2/AgNPs) sample starting from 400 nm showing peak value around 550 nm and ending at higher wavelength values can clearly be seen. Similarly, a negative trend in TCR for 99 nm thickness (TiO_2/AgNPs) substrates indicates a large decrease in the transmission when exposed to CO_2 gas atmosphere. Again a perturbation starting from 460 nm and ending at higher wavelength values can be observed. From these TCR results, it can be inferred that enhanced TiO_2 film thickness decorated with AgNPs confirmed effectiveness of hetero-nanostructures for good CO_2 gas sensors.

3.3.6. Optical Sensing Mechanism for CO_2 Gas. The interaction of gases with solid surfaces depends on various factors such as the type of the gas (reducing or oxidizing in nature), chemical nature of solid surface (n-type or p-type), surface morphology, and the surrounding atmosphere including temperature and humidity [29–31]. Furthermore, type of sensing layers' configuration, whether a single component-based nanostructure or a multimaterial hetero-nanostructure, also plays a vital role to control surface reactions and thus gas-sensing mechanism [15].

TiO_2 is an n-type semiconducting material having d^0 electronic configuration and belongs to the binary transition metal oxide category which is considered potential candidate for real gas-sensing applications. The gas-sensing mechanism of TiO_2-based sensors can be described by considering the adsorption of oxygen on the surface of sensors which could be due to physisorption and chemisorption processes. These processes are found to be surface temperature and activation energy dependent. When TiO_2-based sensors are exposed to air at room temperature, oxygen molecules may adsorb on the surface of TiO_2-based materials by

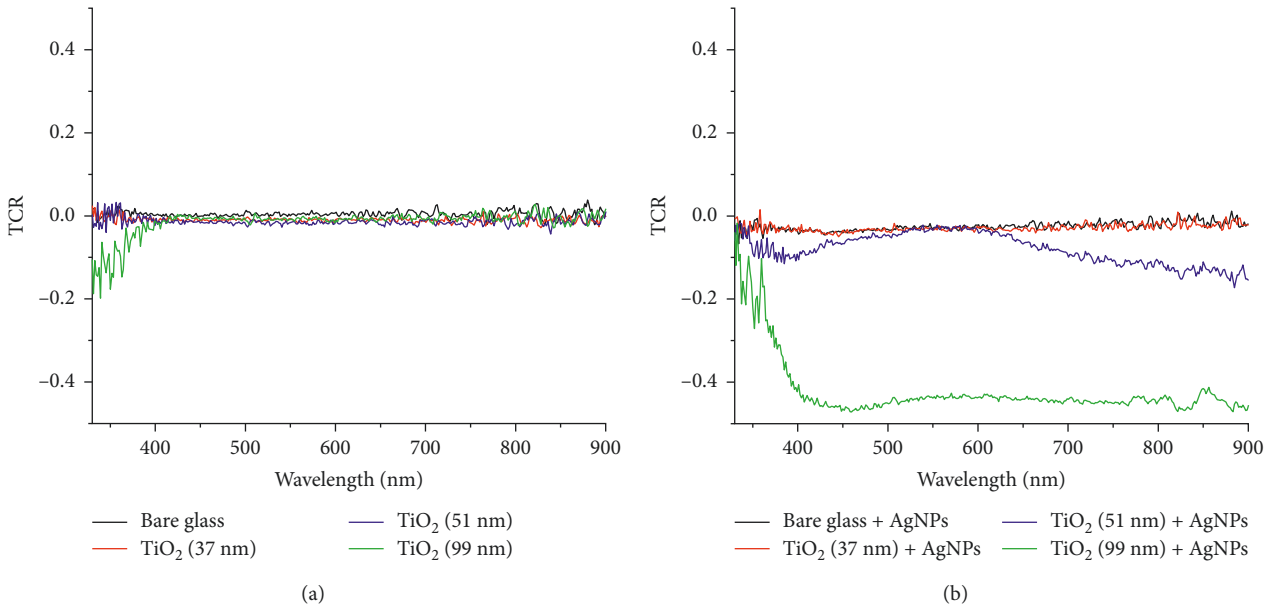

Figure 12: TCR of TiO_2 thin films without (a) and with AgNPs (b).

physisorption process due to Van der Waals and dipole interactions. These adsorbed oxygen molecules, then, generate chemisorbed oxygen species (O_2^-) on the sensor surfaces. The reaction process can be described as follows [15, 30]:

$$\begin{aligned} O_2\,(g) &\longrightarrow O_2\,(ads) \\ O_2\,(ads) + e &\longrightarrow O_2^- \end{aligned} \tag{3}$$

Carbon dioxide (CO_2) is an oxidizing gas having a linear bonded atoms' stable structure with no lone pair of electrons. When TiO_2-based surfaces are exposed to CO_2 gaseous atmosphere at room temperature, the moisture present on the surface of sensor come into action. The water molecules split into hydroxyl and hydrogen ions which subsequently react with gaseous CO_2 to form carbonate ions as follows [31]:

$$\begin{aligned} CO_{2\,(gas)} + OH^-_{(adsorbed)} &\rightleftharpoons HCO^-_{3\,(surface)} \\ CO_{2\,(gas)} + H^+_{(adsorbed)} + 2e^-_{(surface)} &\longrightarrow HCO^-_{2\,(surface)} \\ HCO^-_{2\,(surface)} &\longrightarrow CO\uparrow + OH^-_{(surface)} \\ HCO^-_{3\,(surface)} + OH^-_{(absorbed)} &\rightleftharpoons CO^{2-}_{3\,(bulk)} + H_2O_{(gas)} \end{aligned} \tag{4}$$

TiO_2-based gas sensor properties are also influenced by the TiO_2 crystal phases, and rutile and anatase phases are found to be more promising for the sensing applications.

In our case, alone pristine TiO_2 thin films even with increased film thickness (37–99 nm) exposed to CO_2 gaseous flow could not exhibit any notable sensing performance (Figures 10(a)–10(c)). One of the probable reasons of this little or no sensing response of as-deposited TiO_2 films could be the lack of TiO_2 crystalline phases (Figure 5(a)) or higher sensitivity of TiO_2 polymorph toward reducing gases (such as CO and H_2) than oxidizing gases such as CO_2 [17, 29]. Besides, negligible CO_2 gas-sensing properties of alone AgNP substrates (Figure 10(a)) suggested that neither alone as-deposited TiO_2 thin films nor alone AgNPs were substantial materials for CO_2 gas-sensing mechanism. Instead, hetero-structure fabricated by decorating AgNPs on the predeposited TiO_2 thin films demonstrated excellent CO_2 gas sensing (Figure 12(b)). Manera et al. [12] in the case of alcohol vapor sensors using TiO_2/gold nanocomposite and Wang et al. [30] during their CO gas-sensing studies have already reported the significance of hetero-nanostructures in improving the gas-sensing properties.

This enhanced gas-sensing abilities of our TiO_2/AgNPs hetero-structured sensors can be explained in the way that introduction of silver nanoentities on the TiO_2 films generated high oxygen dissociation active sites which increased the probability of CO_2 adsorption and reaction on the sensor surfaces [15, 32]. This perhaps provoked the prominent change in optical transmission when sensors exposed to in CO_2 gaseous environment. Furthermore, enhanced adsorption of CO_2 near the AgNPs could lead the changes in the refractive index of TiO_2 [33] which caused a change in optical response. Another reason of improved sensing effect due to AgNPs on the TiO_2 films could be the surface plasmon resonance (SPR) effect which is influenced by the variation in thickness and refractive index of the active sensing layer. Moreover, the size and density of AgNP islands on the TiO_2 films could also affect the SPR gas sensitivity [33, 34]. The increased CO_2 sensing properties of TiO_2 films decorated with AgNPs with higher film thickness could be due to the enhanced SPR effect owing to increasing the thickness of TiO_2 film along with growing size and density of AgNP islands.

Thus findings of this work proved that TiO_2/AgNPs hetero-nanostructures were more efficient CO_2 gas optical sensors rather than alone AgNPs or as-deposited TiO_2 films. The excellence performance of prepared hetero-nanostructured CO_2 gas sensors makes them promising candidates for practical gas-sensing applications.

4. Conclusion

In summary, CO_2 gas-sensing characteristics of different substrates including alone AgNPs, TiO_2 thin films with different thickness prepared by different sputtering times and TiO_2/AgNPs hetero-nanostructures were studied. The surface morphology of all the samples was determined by SEM and TiO_2 film thickness and roughness was found enhancing by increasing film sputtering times. The deposition of AgNPs introduced the Ag islands on the TiO_2 films and thus further increased the surface roughness. XRD investigations confirmed the amorphous nature of TiO_2 thin films and FCC crystalline structure of AgNPs. By ellipsometry measurement using Tauc–Lorentz model, film thickness was found to be 37 nm, 51 nm, and 99 nm for sputtering times of 30 min, 60 min, and 90 min, respectively. Optical CO_2 gas detection studies, performed by ellipsometry in alone air and CO_2 gas flow, showed that only TiO_2/AgNPs hetero-nanostructures exhibited substantial sensing performance as compared to single component-based structures. These results revealed the vital role of hetero-nanostructures in improving the gas-sensing properties by virtue of synergistic effects.

Data Availability

All the data and references cited to support our results are available and can be found on the internet.

Disclosure

Some part of this work has been presented at International Conference on Solid State Physics (ICSSP'17), December 10–14, Lahore, Pakistan.

Conflicts of Interest

The authors declare that they have no conflicts of interest.

Acknowledgments

The authors highly acknowledge the financial support provided the Higher Education Commission (HEC) of Pakistan and Centre of Excellence in Solid State Physics, University of the Punjab, QAC, Lahore 54590, Pakistan.

References

[1] M. U. Qadri, A. F. Diaz, M. Cittadini et al., "Effect of pt nanoparticles on the optical gas sensing properties of WO_3 thin films," *Sensors*, vol. 14, no. 7, pp. 11427–11443, 2014.

[2] B. Yuliarto, G. Gumilar, and N. W. Septiani, "SnO_2 nanostructure as pollutant gas sensors: synthesis, sensing performances, and mechanism," *Advances in Materials Science and Engineering*, vol. 2015, Article ID 694823, 14 pages, 2015.

[3] J. Hodgkinson and R. P. Tatam, "Optical gas sensing: a review," *Measurement Science and Technology*, vol. 24, no. 1, p. 012004, 2013.

[4] E. Bakker and M. Telting-Diaz, "Electrochemical sensors," *Analytical Chemistry*, vol. 74, no. 12, pp. 2781–800, 2002.

[5] M. Lackner, "Tunable diode laser absorption spectroscopy (TDLAS) in the process industries—a review," *Reviews in Chemical Engineering*, vol. 23, no. 2, pp. 65–147, 2007.

[6] E. D. Gaspera and A. Martucci, "Sol-gel thin films for plasmonic gas sensors," *Sensors*, vol. 15, no. 7, pp. 16910–16928, 2015.

[7] J. Wang, Z. Wen, B. Yang, and X. Yang, "Optical carbon dioxide sensor based on fluorescent capillary array," *Results in Physics*, vol. 7, pp. 323–326, 2017.

[8] J. Sun, B. Ye, G. Xia, X. Zhao, and H. Wang, "A colorimetric and fluorescent chemosensor for the highly sensitive detection of CO_2 gas: experiment and DFT calculation," *Sensors and Actuators B*, vol. 233, pp. 76–82, 2016.

[9] P. K. Contreras-Gutierrez, S. Medina-Rodríguez, A. L. Medina-Castillo, J. F. Fernandez-Sanchez, and A. Fernandez-Gutierrez, "A new highly sensitive and versatile optical sensing film for controlling CO_2 in gaseous and aqueous media," *Sensors and Actuators B*, vol. 184, pp. 281–287, 2013.

[10] I. M. P. Vargas-Sansalvador, M. A. Carvajal, O. M. Roldan-Munoz, J. Banqueri, M. D. Fernandez-Ramos, and L. F. Capitan-Vallvey, "Phosphorescent sensing of carbon dioxide based on secondary inner-filter quenching," *Analytica Chimica Acta*, vol. 655, no. 1-2, pp. 66–74, 2009.

[11] L. Lochman, P. Zimcik, I. Klimant, V. Novakova, and S. M. Borisov, "Red-emitting CO_2 sensors with tunable dynamic range based on pH-sensitive azaphthalocyanine indicators," *Sensors and Actuators B*, vol. 246, pp. 1100–1107, 2017.

[12] M. G. Manera, J. Spadavecclia, D. Buso et al., "Optical gas sensing of TiO_2 and TiO_2/Au nanocomposite thin films," *Sensors and Actuators B*, vol. 132, no. 1, pp. 107–115, 2008.

[13] K. R. Nemade and S. A. Waghuley, "Comparative study of carbon dioxide sensing by Sn-doped TiO_2 nanoparticles synthesized by microwave-assisted and solid-state diffusion route," *Applied Nanoscience*, vol. 5, no. 4, pp. 419–424, 2015.

[14] Y. Tashiro, S. Komasa, A. Miyake, H. Nishizaki, and J. Okazaki, "Analysis of titania nanosheet adsorption behavior using a quartz crystal microbalance sensor," *Advances in Materials Science and Engineering*, vol. 2018, Article ID 7461245, 10 pages, 2018.

[15] Y. Wang, T. Wu, Y. Zhou, C. Meng, W. Zhu, and L. Liu, "TiO_2-based nanoheterostructures for promoting gas sensitivity performance: designs, developments, and prospects," *Sensors*, vol. 17, no. 9, p. 1971, 2017.

[16] S. Islam, N. Bidin, S. Riaz, R. A. Rahman, S. Naseem, and F. M. Marsin, "Mesoporous SiO_2–TiO_2 nanocomposite for pH sensing," *Sensors and Actuators B*, vol. 221, pp. 993–1002, 2015.

[17] E. D. Gaspera, D. Buso, M. L. Post, and A. Martucci, "TiO_2 sol-gel thin films containing Au and Pt nanoparticles with controlled morphology: optical study and gas sensing properties," in *Proceedings of Optical Sensing and Detection–SPIE*, Brussels, Belgium, May 2010.

[18] E. D. Gaspera, M. Bersani, G. Mattei, T. L. Nguyen, P. Mulvaney, and A. Martucci, "Cooperative effect of Au and Pt inside TiO_2 matrix for optical hydrogen detection at room temperature using surface plasmon spectroscopy," *Nanoscale*, vol. 4, no. 19, pp. 5972–5979, 2012.

[19] M. A. Raza, Z. Kanwal, A. Rauf, A. N. Sabri, S. Riaz, and S. Nasim, "Size- and shape-dependent antibacterial studies of silver nanoparticles synthesized by wet chemical routes," *Nanomaterials*, vol. 6, no. 4, p. 74, 2016.

[20] A. A. El-Kheshen and S. F. G. El-Rab, "Effect of reducing and protecting agents on size of silver nanoparticles and their antibacterial activity," *Pharmaceutical Chemistry*, vol. 4, pp. 53–65, 2012.

[21] M. T. J. van Loenhout, E. S. Kooij, H. Wormeester, and B. Poelsema, "Hydrodynamic flow induced anisotropy in colloid adsorption," *Colloids and Surfaces A: Physicochemical and Engineering Aspects*, vol. 342, no. 1–3, pp. 46–52, 2009.

[22] K. Jyoti, M. Banuthiyal, and A. Singh, "Characterization of silver nanoparticles synthesized using Urtica diocia linn leaves and their synergistic effects with antibiotics," *Journal of Radiation Research and Applied Sciences*, vol. 9, no. 3, pp. 217–227, 2016.

[23] B. Parveen, M. Hassan, S. Atiq, S. Riaz, S. Naseem, and S. Zaman, "Structural, dielectric and ferromagnetic properties of nano-crystalline Co-doped SnS," *Journal of Materials Science*, vol. 52, no. 12, pp. 7369–7381, 2017.

[24] N. Laidani, R. Bartali, G. Gottardi, M. Anderle, and P. Cheyssac, "Optical absorption parameters of amorphous carbon films from Forouhi–Bloomer and Tauc–Lorentz models: a comparative study," *Journal of Physics: Condensed Matter*, vol. 20, no. 1, pp. 015216.l–015216.8, 2008.

[25] F. Hanini, B. Bouabellou, Y. Bouachiba et al., "Structural, optical and electrical properties of TiO_2 thin films synthesized by sol–gel technique," *ISOR Journal of Engineering*, vol. 3, no. 11, pp. 21–28, 2013.

[26] M. Farzana, R. Saira, and N. Shahzad, "Optical properties of Electrodeposited alumina thin films by using Spectroscopic Ellipsometer," *Applied Mechanics and Materials*, vol. 319, pp. 84–89, 2013.

[27] D. Meroni, L. Lo Presti, G. Di Liberto et al., "A close look at the structure of the TiO_2-APTES interface in hybrid nanomaterials and its degradation pathway: an experimental and theoretical study," *Journal of Physical Chemistry*, vol. 121, no. 1, pp. 430–440, 2017.

[28] M. Baum, J. Strauß, F Grüßel, I. Alexeev, and M. Schmidt, "Generation of phase-only holograms by laser ablation of nanoparticulate ITO layers," *Journal of Optics*, vol. 16, no. 12, p. 125706, 2014.

[29] H. H. Hamdan and G. H. Mohammed, "Hydrogen gas sensing properties of AgNPs-doped titania nanotubes by electroless deposition," *International Journal of Science and Research (IJSR)*, vol. 5, no. 2, pp. 2224–2233, 2016.

[30] C. Wang, L. Yin, L. Zhang, D. Xiang, and R. Gao, "Metal oxide gas sensors: sensitivity and influencing factors," *Sensors*, vol. 10, no. 3, pp. 2088–2106, 2010.

[31] P. Shankar and J. B. B. Rayappan, "Gas sensing mechanism of metal oxides: the role of ambient atmosphere, type of semiconductor and gases–A review," *Science Letters Journal*, vol. 4, p. 26, 2015.

[32] A. S. M. Iftekhar Uddin, D. T. Phan, and G. S. Chung, "Low temperature acetylene gas sensor based on Ag nanoparticles-loaded ZnO-reduced graphene oxide hybrid," *Sensors and Actuators B*, vol. 207, pp. 362–369, 2015.

[33] D. Buso, M. Post, C. Cantalini, P. Mulvaney, and A. Martucci, "Gold nanoparticle-doped TiO_2 semiconductor thin films: gas sensing properties," *Advanced Functional Materials*, vol. 18, no. 23, pp. 3843–3849, 2008.

[34] P. I. Gaiduk, J. Chevallier, S. L. Prokopyev, and A. N. Larsen, "Plasmonic-based SnO_2 gas sensor with in-void segregated silver nanoparticles," *Microelectronic Engineering*, vol. 125, pp. 68–72, 2014.